

Supporting Information

The Pentavalent Lanthanide Nitride-Oxides: NPrO and NPrO⁻ Complexes with N≡Pr Triple Bonds

Shuxian Hu,^{1,2} Jiwen Jian,³ Jing Su,² Xuan Wu,³ Jun Li^{2*} and Mingfei Zhou^{3*}

¹ Beijing Computational Science Research Center, Beijing 100094, China.

² Department of Chemistry and Key Laboratory of Organic Optoelectronics & Molecular Engineering of Ministry of Education, Tsinghua University, Beijing 100084, China.

³ Collaborative Innovation Center of Chemistry for Energy Materials, Department of Chemistry, Shanghai Key Laboratory of Molecular Catalysis and Innovative Materials, Fudan University, Shanghai 200433, China.

Table S1. Product absorption (cm⁻¹) from co-deposition of laser-ablated Pr Atoms with NO in solid neon.

¹⁴ NO	¹⁵ NO	R _{14/15}	assignment
926.2/918.5 762.2/755.9	903.9/896.6 757.0/750.7	1.0247/1.0244 1.0069/1.0069	NPrO
730.9 623.9	709.2 623.8	1.0306 1.0002	NPrO ⁻
1862.6 886.6 751.6	1829.8 868.6 744.5	1.0179 1.0207 1.0095	NPrO(NO)
1825.4 1720.6 826.3	1793.4 1690.2 817.2	1.0178 1.0180 1.0111	NPrO(NO) ₂
747.3	747.3	1.0000	PrO ₂ (N ₂)

Table S2. Total binding energies (kcal/mol) of the NPrO(Ng)_x (Ng = Ne, Ar) and NPrO(NO)_x complexes calculated at B3LYP level with and without the dispersion correction.

<i>x</i>	B3LYP			B3LYP-D3		
	Ne	Ar	NO	Ne	Ar	NO
1	-0.65	-0.86	-8.90	-3.30	-4.45	-13.56
2	-0.76	-1.14	-15.80	-4.06	-6.28	-24.41
3	-0.88	-1.45		-4.81	-8.18	
4	-0.93	-1.66		-5.54	-10.23	
5	-0.96	-1.36		-6.27	-12.11	
6	-0.95	-0.54		-7.19	-12.66	
7	-0.65			-0.52	-0.06	

Table S3. The calculated natural localized molecular orbitals (NLMOs) of NPrO and NPrO⁻.

Species	Type	Occ.	NLMO
NPrO	$\sigma_{\text{Pr-N}}$	2.0	60.9%Pr(21%d+74%f) + 36.8%N(13%s+87%p)
	$\pi_{\text{Pr-N}}$	4.0	32.5%Pr(41%d+58%f) + 67.5%N(100%p)
	$\sigma_{\text{Pr-O}}$	2.0	30.9%Pr(26%d+71%f) + 67.3%O(13%s+87%p)
	$\pi_{\text{Pr-O}}$	4.0	17.1%Pr(44%d+55%f) + 82.8%O(100%p)
NPrO ⁻	$\sigma_{\text{Pr-N}}$	2.0	59.8%Pr(36%s+22%d+41%f) + 38.6%N(4%s+96%p)
	$\pi_{\text{Pr-N}}$	4.0	24.3%Pr(55%d+43%f) + 75.7%N(100%p)
	$\sigma_{\text{Pr-O}}$	2.0	21.6%Pr(6%s+18%d+74%f) + 76.9%O(13%s+87%p)
	$\pi_{\text{Pr-O}}$	4.0	13.7%Pr(54%d+42%f) + 86.3%O(100%p)

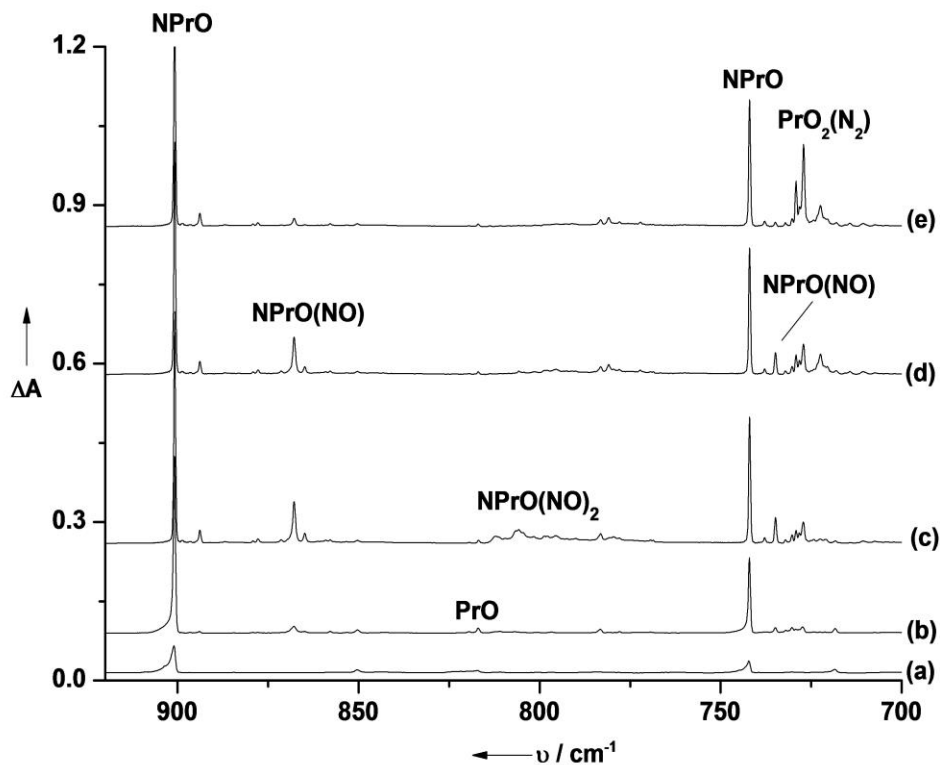


Figure S1. Infrared spectra in the 920-700 cm^{-1} region from co-deposition of praseodymium atoms with 0.1% NO in argon. (a) after 1 h of sample deposition at 4 K, (b) after annealing to 20 K, (c) after annealing to 30 K, (d) after 15 min of $\lambda > 800 \text{ nm}$ irradiation, and (e) after 15 min of $\lambda > 700 \text{ nm}$ irradiation.

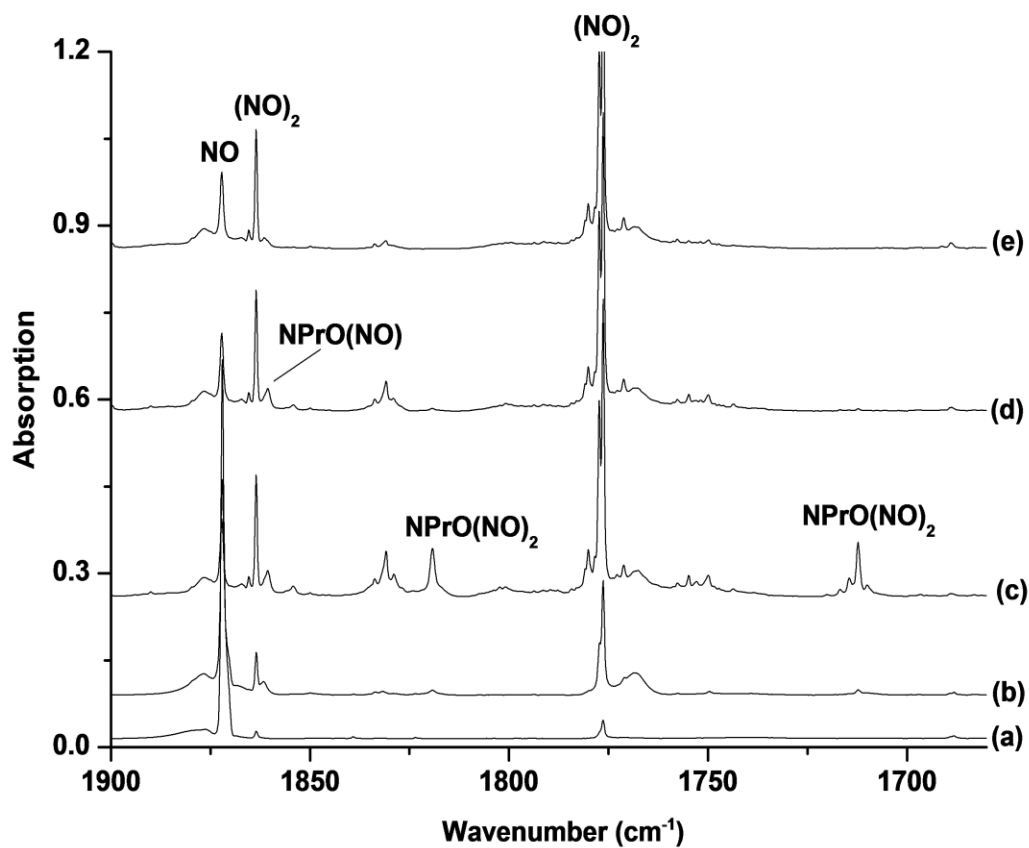


Figure S2. Infrared spectra in the 1900-1680 cm⁻¹ region from co-deposition of praseodymium atoms with 0.1% NO in argon. (a) after 1 h of sample deposition at 4 K, (b) after annealing to 20 K, (c) after annealing to 30 K, (d) after 15 min of 1 > 800 nm irradiation, and (e) after 15 min of 1 > 700nm irradiation.

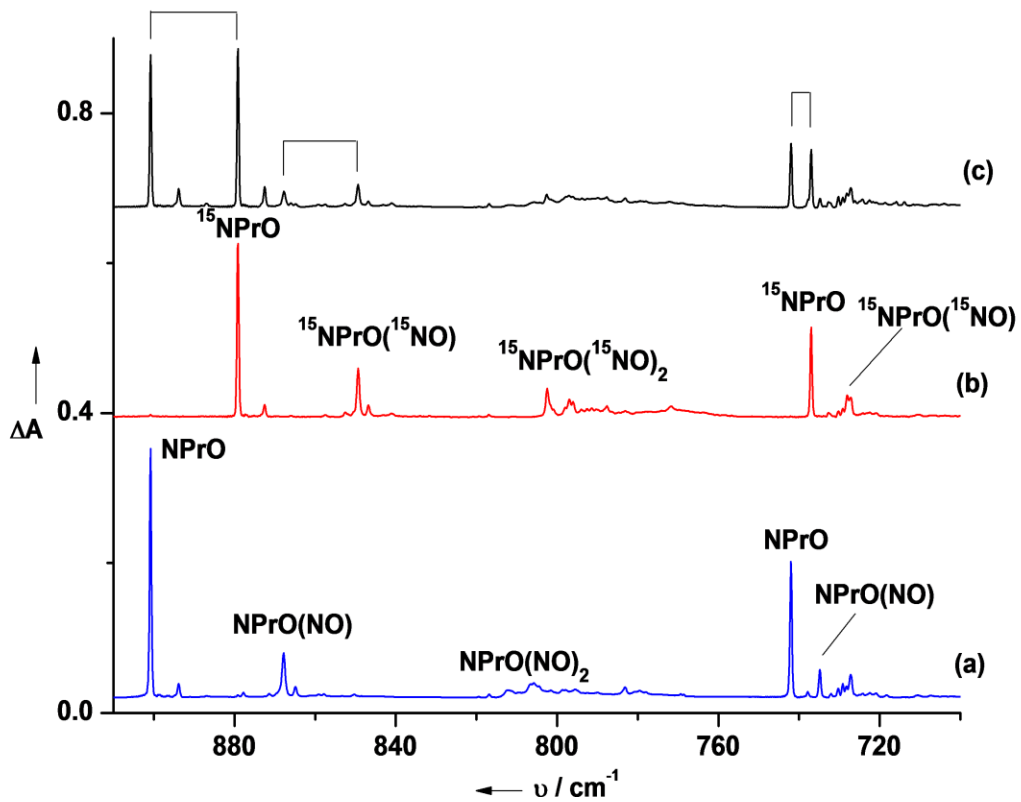


Figure S3. Infrared spectra in the 920-700 cm^{-1} region from co-deposition of praseodymium atoms with isotopic-labeled NO in excess argon. Spectrum was taken after 30 K annealing. (a) 0.1% ^{14}NO , (b) 0.1% ^{15}NO , and (c) 0.05% ^{14}NO + 0.05% ^{15}NO .

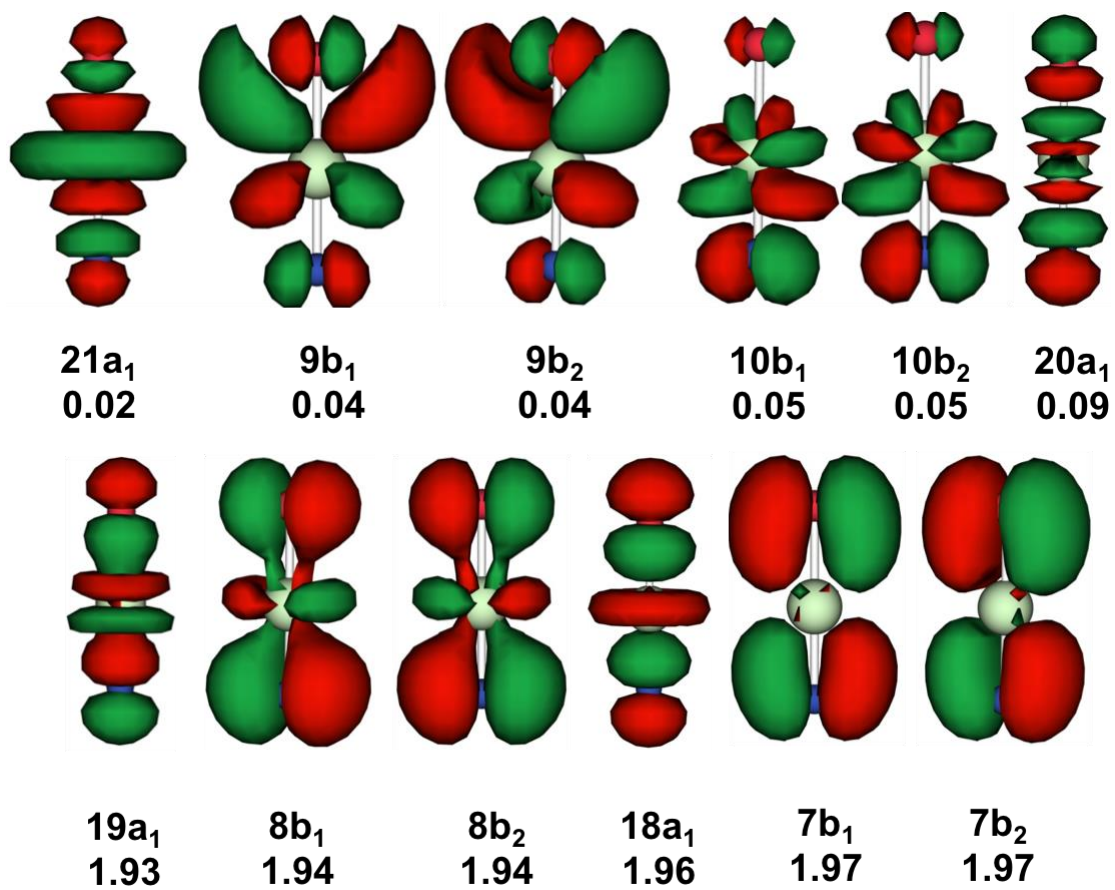


Figure S4. NOONs and natural orbitals of NPrO from CASSCF (12,12)/VDZP calculations.

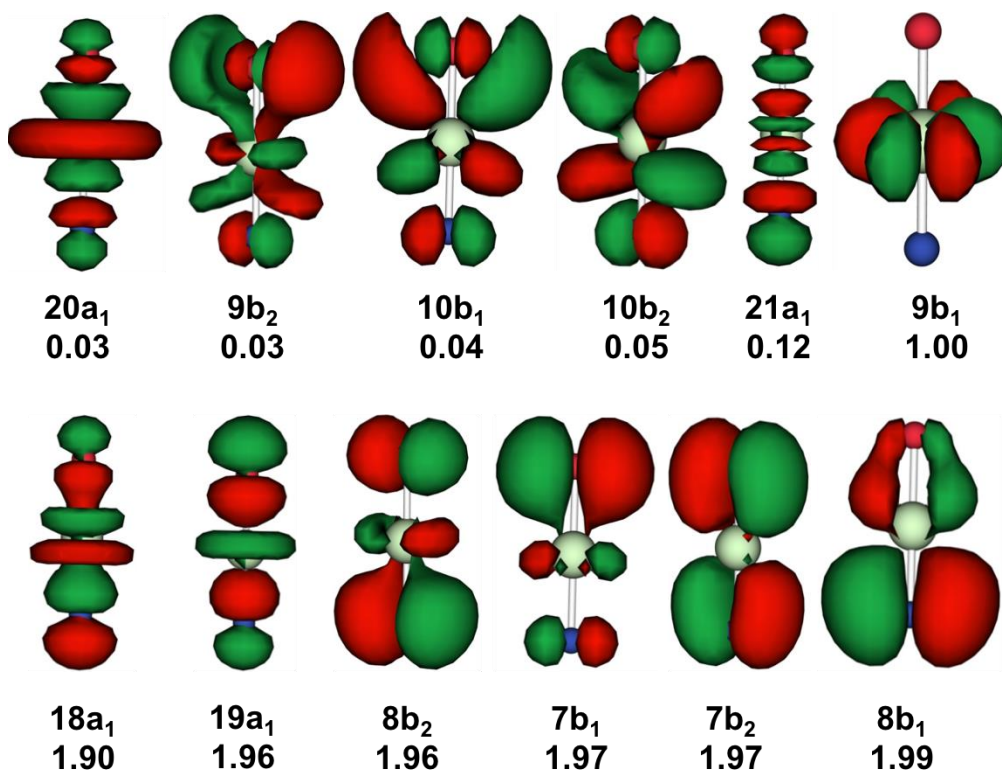


Figure S5. NOONs and natural orbitals of NPrO⁻ from CASSCF (13,12)/VDZP calculations.

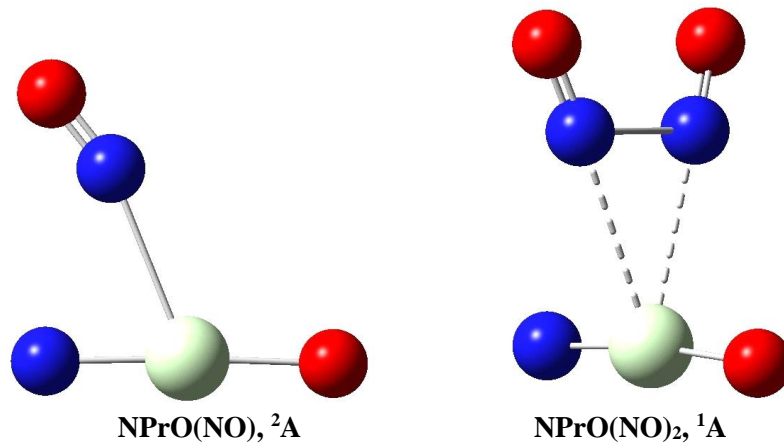


Figure S6. Optimized structures of the NPrO(NO) and NPrO(NO)₂ complexes.

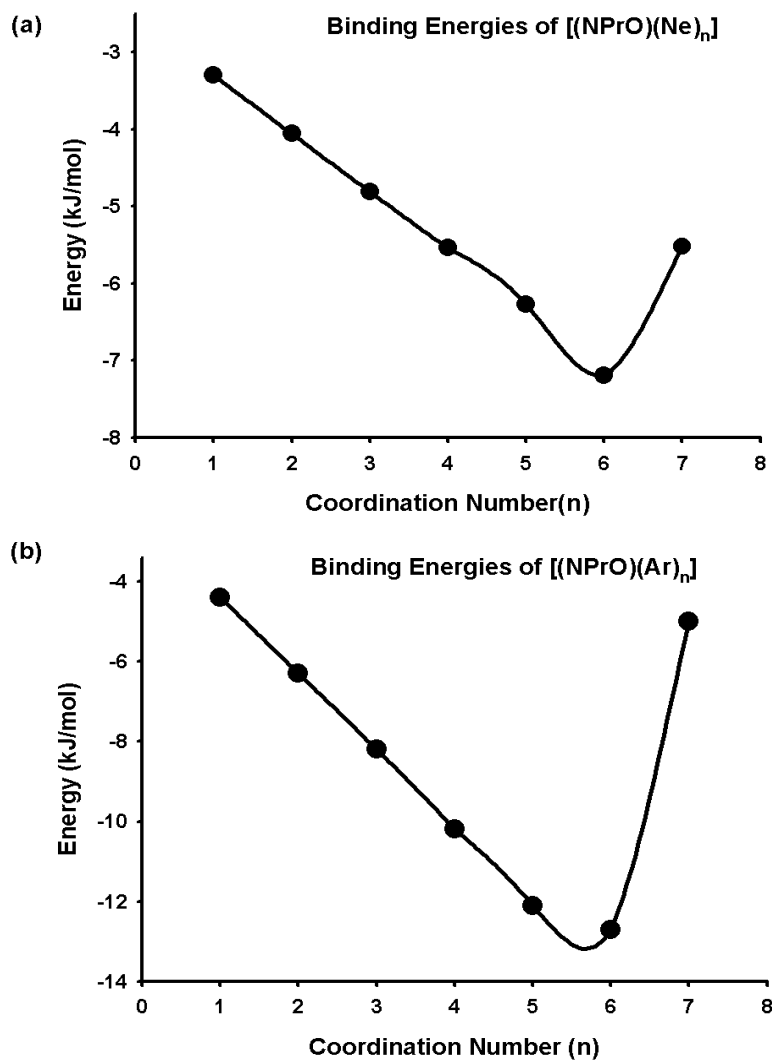


Figure S7. Total binding energies of $[\text{NPrO}(\text{Ng})_n]$ ($\text{Ng} = \text{Ne}, \text{Ar}$) calculated at DFT/B3LYP-D3 level.